

On the Correlation between Hot Jupiters and Stellar Clustering: High-Eccentricity Migration Induced by Stellar Flybys

LAETITIA RODET,¹ YUBO SU,¹ AND DONG LAI¹

¹*Cornell Center for Astrophysics and Planetary Science, Department of Astronomy, Cornell University, Ithaca, NY 14853, USA*

ABSTRACT

A recent observational study suggests that the occurrence of hot Jupiters (HJs) around solar type stars is correlated with stellar clustering. We study a new scenario for HJ formation, called “Flyby Induced High-e Migration”, that may help explain this correlation. In this scenario, stellar flybys excite the eccentricity and inclination of an outer planet (or brown dwarf) at large distance (10-300 au), which then triggers high-e migration of an inner cold Jupiter (at a few au) through the combined effects of von Zeipel-Lidov-Kozai (ZLK) eccentricity oscillation and tidal dissipation. Using semi-analytical calculations of the effective ZLK inclination window, together with numerical simulations of stellar flybys, we obtain the analytic estimate for the HJ occurrence rate in this formation scenario. We find that this “flyby induced high-e migration” could account for a significant fraction of the observed HJ population, although the result depends on several uncertain parameters, including the density and lifetime of birth stellar clusters, and the occurrence rate of the “cold Jupiter + outer planet” systems.

Keywords: Hot Jupiters — Close Encounters — Exoplanet dynamics

1. INTRODUCTION

Hot Jupiters (HJs), giant planets orbiting with very-short period (~ 3 days) are found around 1% of FGK stars (see Dawson & Johnson 2018, and references therein). HJs can form in three ways: in-situ, through disk-driven migration or high-eccentricity migration. There is currently no consensus on the predominant channel for their origin.

Recent work by Winter et al. (2020) has revealed an intriguing correlation between the occurrence of HJs and stellar clustering. For each exoplanet-hosting star in their sample, the authors computed the local stellar phase-space density of the star and its neighbors (within 40 pc) using Gaia DR2 (Gaia Collaboration et al. 2018). They determined whether the exoplanet host was in a relatively low or high stellar density zone compared to its neighbours, and concluded that HJs were preferably found in local stellar phase-space overdensities. The origin of this correlation is puzzling, as stellar clustering was thought to affect mostly the outer part of planetary systems in very dense environments (Laughlin & Adams

1998; Malmberg et al. 2011; Parker & Quanz 2012; Cai et al. 2017; Li et al. 2020).

The formation of HJs in-situ or through disk-driven migration is not directly correlated to the stellar environment. However, high-e migration may correlate with stellar density. This mechanism relies on the excitation of a cold Jupiter’s eccentricity by an outer perturber. The semi-major axis of the planet is then decreased by tidal dissipation at each periastron passage (e.g., Wu & Murray 2003; Fabrycky & Tremaine 2007; Nagasawa et al. 2008; Naoz et al. 2012; Wu & Lithwick 2011; Beaugé & Nesvorný 2012; Petrovich 2015a,b; Anderson et al. 2016; Vick et al. 2019; Teyssandier et al. 2019). The occurrence rate of this formation path may depend on the frequency of stellar flybys, through dynamical interactions between the passing stars and the outer planetary system (e.g.; Shara et al. 2016). In Wang et al. (2020), the authors considered a scenario where a stellar flyby excites an outer Saturn, which in turn raises the eccentricity of the inner Jupiter by planet-planet scattering or through the von Zeipel-Lidov-Kozai (ZLK, von Zeipel 1910; Lidov 1962; Kozai 1962) mechanism. They estimated numerically the resulting occurrence rate of HJs in a virialized cluster, and showed that this formation path has a negligible rate. However, this study is restricted to specific ranges of cluster parameters and

initial planetary systems, and the numerical approach limits the generality of the results.

In this paper, we examine the likelihood of HJs forming through high- e migration triggered by flybys in a stellar environment, using a combination of analytical calculations (for high- e migration) and numerical simulations (for stellar flybys). In Section 2 we outline the proposed scenario and its key ingredients. In Section 3, we review the conditions for the ZLK mechanism to produce a HJ, and extend previous works to examine the case of a planetary-mass perturber. In Section 4, we evaluate the extent to which a stellar encounter can raise the eccentricity and inclination of an outer planet. In Section 5, we derive the occurrence rate of HJs as a function of the properties of the system and its stellar neighborhood. Finally, in Section 6, we conclude and discuss alternative explanations for the observed correlations between HJs and stellar overdensities.

2. FLYBY INDUCED HIGH-E MIGRATION SCENARIO

According to the current understanding of planetary formation, giant planets form preferentially beyond the snow line at a few astronomical units. Their migration to the close neighborhoods of their host stars can be triggered by a combination of eccentricity excitation and tidal dissipation—the so-called high- e migration mechanism (see references in Section 1). This requires the presence of a misaligned and eccentric outer perturber (see Section 3). To evaluate the probability to form HJs through high- e migration, we thus need to estimate the occurrence rate of such perturbers.

On one hand, misaligned perturbers could be naturally associated with binary companions. The orientation of stellar companions with respect to the protoplanetary disk plane of the primary is expected to be random at large separations. This is also likely the case for at least some fraction of the substellar companions (brown dwarfs). This possibility is examined in Section 6.

On the other hand, a scattering encounter between a planetary system and a passing star could raise the eccentricity and inclination of an initially coplanar and circular outer body, which then drives the inner cold Jupiter into a high- e orbit, leading to HJ formation. The probability of this HJ formation channel is strongly dependent on the stellar density. The combination of flyby and high- e migration could account for the observed correlation between HJ occurrence and stellar overdensity. High- e migration can be triggered by the ZLK mechanism or by planet-planet scattering. This paper will focus on the former, and the latter is discussed in Section 6.

For the basic setup, we consider two giant planets around a solar-type star (with mass M_1), an inner cold Jupiter (m_J) at $a_J \sim 5$ au and an outer planet/perturber (m_p) at larger separations ($a_p \in 10$ –500 au). We assume that the initial planetary orbits are coplanar and circular, as is expected from their formation in a gaseous protoplanetary disk. We consider a passing star (M_2) with velocity at infinity v_∞ and periastron q . In the following sections, we will examine the requirements for the passing star to trigger the high- e migration of the cold Jupiter via excitation of the outer planet’s orbit.

3. EFFECTIVE RANGE OF ZLK ECCENTRICITY EXCITATION AND HIGH-E MIGRATION

3.1. Semi-major axis window

Not every semi-major axis ratio a_J/a_p can lead to the formation of HJs. High- e migration requires the inner planet (m_J) to attain a sufficiently large eccentricity. The maximum eccentricity depends on i_p , the mutual inclination between the planet and the perturber (m_p), and the competition between eccentricity driving by the ZLK mechanism and its suppression due to short-range forces (e.g., Fabrycky & Tremaine 2007; Liu et al. 2015, hereafter LML15). In our case, the most important of these forces is the tidal force from the star on the inner planet. Over all possible values of i_p , the inner planet cannot become more eccentric than the limiting eccentricity e_{lim} , as determined by LML15:

$$\frac{\dot{\omega}_{\text{tides}}}{\dot{\omega}_{\text{ZLK}}}\Big|_{e_J=e_{\text{lim}}} = \frac{81}{8}, \quad (1)$$

where $\dot{\omega}_{\text{tides}}$ and $\dot{\omega}_{\text{ZLK}}$ are the precession frequencies due to the tidal force and ZLK mechanism, respectively. They are given by:

$$\dot{\omega}_{\text{tides}} = \frac{15}{2} k_{2,J} \frac{M_1}{m_J} \left(\frac{R_J}{a_J} \right)^5 \frac{1 + \frac{3}{2} e_J^2 + \frac{1}{8} e_J^4}{(1 - e_J^2)^5} n_J, \quad (2)$$

$$\dot{\omega}_{\text{ZLK}} = \frac{m_p}{M_1} \left(\frac{a_J}{a_{p,\text{eff}}} \right)^3 \frac{n_J}{\sqrt{1 - e_J^2}}, \quad (3)$$

where $a_{p,\text{eff}} = a_p \sqrt{1 - e_p^2}$, $k_{2,J}$ is the tidal Love number of the planet, R_J its radius and $n_J \equiv \sqrt{GM_1/a_J^3}$ its mean motion. We find

$$\begin{aligned} 1 - e_{\text{lim}} &\approx 10^{-3} \left(\frac{k_{2,J}}{0.37} \right)^{\frac{2}{9}} \left(\frac{R_J}{1 R_{\text{Jup}}} \right)^{\frac{10}{9}} \left(\frac{a_{p,\text{eff}}}{40 \text{ au}} \right)^{\frac{2}{3}} \\ &\times \left(\frac{m_p}{5 M_{\text{Jup}}} \right)^{-\frac{2}{9}} \left(\frac{m_J}{1 M_{\text{Jup}}} \right)^{-\frac{2}{9}} \\ &\times \left(\frac{M_1}{1 M_\odot} \right)^{\frac{4}{9}} \left(\frac{a_J}{5 \text{ au}} \right)^{-\frac{16}{9}}. \end{aligned} \quad (4)$$

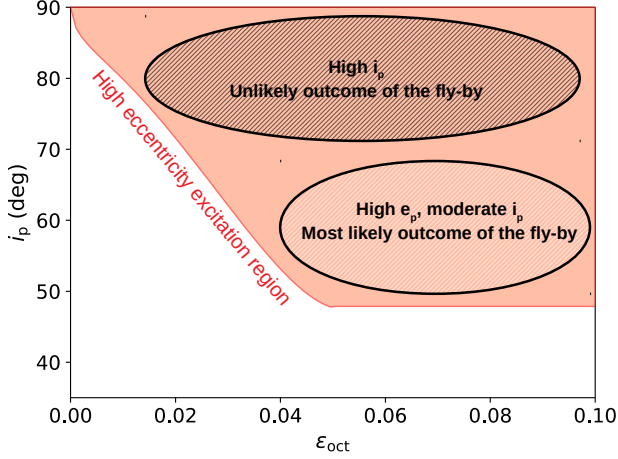


Figure 1. High eccentricity excitation region for the inner planet in the ZLK problem at the octupole order, in the $\varepsilon_{\text{oct}}-i_p$ phase space (where i_p is the inclination of the external perturber, and ε_{oct} is given by Eq. 6). The boundary of the light red zone is given by the fitting formula of Muñoz et al. (2016), and systems in this zone can attain extreme eccentricity e_{lim} [Eq. (4)], assuming the inner planet has a negligible angular momentum compared to that of the outer perturber. High inclinations are harder to produce with a flyby than high eccentricities (corresponding to high values of ε_{oct} , see Section 4).

To produce a HJ with a (circular) semi-major axis a_{HJ} (~ 0.04 au, corresponding to a 3-day orbit), we require the pericenter distance $a_J(1 - e_J)$ to reach below $a_{\text{HJ}}/2$. This gives

$$\frac{a_J}{a_{\text{p,eff}}} \gtrsim \frac{1}{50} \left(\frac{k_{2,J}}{0.37} \right)^{\frac{2}{7}} \left(\frac{R_J}{1 R_{\text{Jup}}} \right)^{\frac{10}{7}} \left(\frac{m_J}{1 M_{\text{Jup}}} \right)^{-\frac{2}{7}} \times \left(\frac{M_1}{1 M_{\odot}} \right)^{\frac{4}{7}} \left(\frac{m_p}{5 M_{\text{Jup}}} \right)^{-\frac{2}{7}} \left(\frac{a_{\text{p,eff}}}{40 \text{ au}} \right)^{-\frac{1}{7}} \left(\frac{a_{\text{HJ}}}{0.04 \text{ au}} \right)^{-\frac{9}{7}} \quad (5)$$

The possibility of creating a HJ thus depends mostly on the semi-major axis ratio a_J/a_p , and weakly on a_p alone. For giant planets initially at 5 au and the fiducial parameters, Eq. (5) amounts to $a_{\text{p,eff}} \lesssim 300$ au. As most planets are expected to lie inside this limit, it follows that Eq. (5) does not provide a strong constraint on the semi-major axis of the outer planet/perturber.

3.2. Eccentricity and Inclination window

In the ZLK mechanism, at the quadrupole order, an initially circular planet can only reach extreme eccentricities if the outer perturber’s inclination is close to 90° . This picture is valid under two assumptions: the inner planet is effectively a “test particle” (i.e., its orbital angular momentum is negligible compared to that of the outer perturber) and the octupole-order corrections are sufficiently weak. In the test-particle limit, it has been

shown that the octupole-order effect can induce extreme eccentricities ($e_J \simeq e_{\text{lim}}$) in the inner orbit if the outer orbit’s inclination belongs to a finite window around 90° (LML15; Muñoz et al. 2016, hereafter MLL16) whose size depends on the octupole parameter :

$$\varepsilon_{\text{oct}} = \frac{a_J}{a_p} \frac{e_p}{1 - e_p^2}. \quad (6)$$

As ε_{oct} increases, the inclination window grows until it saturates at $[48^\circ, 132^\circ]$ for $\varepsilon_{\text{oct}} \gtrsim 0.05$ (see Fig. 1). This “symmetric” inclination window is valid in the test-particle limit, when the angular momentum ratio l between the inner planet and the outer perturber is small, i.e.,

$$l \equiv \frac{m_J}{m_p} \sqrt{\frac{a_J(1 - e_J^2)}{a_p(1 - e_p^2)}} \ll 1. \quad (7)$$

However, when both l and ε_{oct} are not negligible, the inclination window obtained by MLL16 cannot predict whether the inner orbit reaches very high eccentricities. To understand the critical value of l below which the prescription of MLL16 is accurate, we have carried out new simulations for the evolution of the inner and outer planetary orbits to octupole-order, using the secular equations given in LML15. We also include general relativistic periastron advance and tidal distortion of the giant planet following LML15. We ignore the orbital decay of the inner planet due to tidal dissipation (which is expected to occur over long timescales). To isolate the impact of different values of l , we vary m_p and a_p such that the quadrupole order ZLK timescale, given by

$$t_{\text{ZLK}}^{-1} \equiv \frac{m_p}{M_1} \left(\frac{a_J}{a_{\text{p,eff}}} \right)^3 n_J, \quad (8)$$

is constant. In particular, we fix $e_p = 0.6$ and the initial $e_J = 10^{-3}$ and consider six values of $m_p = \{1, 2, 3, 5, 10\} \times M_{\text{Jup}}$ and $m_p = M_{\odot}$, while adjusting a_p accordingly. For each value of m_p , we further consider 2000 uniformly spaced initial inclinations $i_p \in [40^\circ, 140^\circ]$. Then, for each inclination, we run three simulations while randomly choosing $\Omega, \omega \in [0, 2\pi)$ for both the inner and outer orbits, the longitude of the ascending node and argument of periapsis respectively, totaling 6000 simulations per combination of m_p and a_p . We run each simulation for $500t_{\text{ZLK}}$ and measure the maximum eccentricity attained by the inner planet. Figure 2 depicts our numerical results. We see that the inclination window predicted by MLL16 is accurate when

$$l \lesssim 0.1. \quad (9)$$

For $l \gtrsim 0.1$, extreme eccentricity can be achieved only for inclinations larger than the test-particle result. As

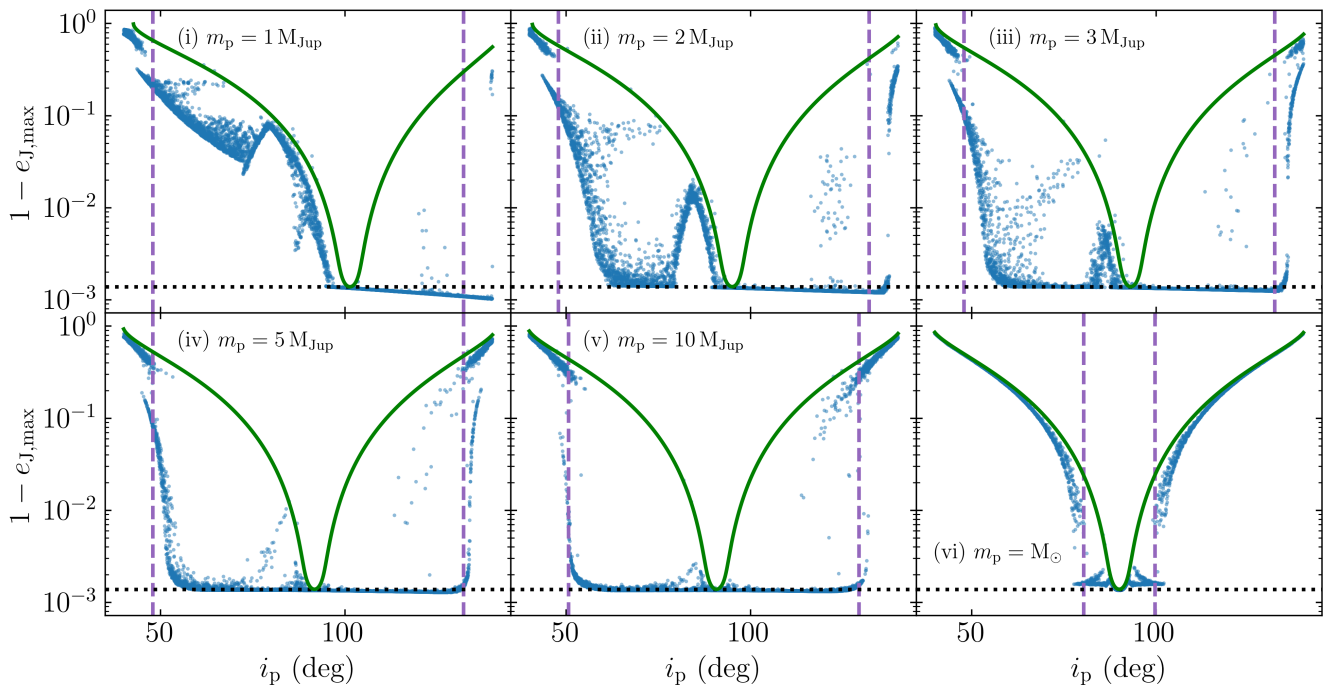


Figure 2. Maximum eccentricity of the inner planet (as $1 - e_{J,\max}$) versus initial inclination i_p for different values of perturber mass m_p (as labelled) and semi-major axis a_p such that t_{ZLK} [Eq. (8)] is held constant ($a_p = 50, 63, 72, 85, 108,$ and 500 au respectively). In all cases, we take $e_p = 0.6$, $M_1 = M_\odot$, $m_J = M_{\text{Jup}}$, $a_J = 5$ AU. The blue dots denote the maximum eccentricities attained by m_J when the system is integrated for $500t_{\text{ZLK}}$. The green line illustrates the analytical $e_{J,\max}(i_p)$ curve when the octupole effect is neglected (see Eq. 50 of LML15). The purple vertical lines denote the inclination window for extreme eccentricity excitation as given by the fitting formula of MLL16 (see Fig. 1 or Eq. 7 of MLL16); for the simulated systems in the six panels, $\varepsilon_{\text{oct}} = 0.09, 0.07, 0.06, 0.05, 0.04,$ and 0.009 respectively. The horizontal dashed line denotes e_{lim} as given by Eq. (4). When $m_p \lesssim 3M_J$, corresponding to $l \gtrsim 0.1$, the angular momentum of the inner planet is nonnegligible, and it is much more difficult for prograde outer planets ($i_p < 90^\circ$) to excite e_J to e_{lim} than it is for retrograde outer planets ($i_p > 90^\circ$).

we shall see in Section 4, for initially coplanar systems, very high inclinations are an unlikely outcome of flybys. Thus, in the following, we will restrict our attention to systems satisfying Eq. (9). Assuming $e_p = 0.6$, this would require $m_p > 4 M_{\text{Jup}}$ for $a_p/a_J = 10$; and $m_p > 2 M_{\text{Jup}}$ for $a_p/a_J = 50$. Note that the limiting eccentricity e_{lim} depends on l^2 (Anderson et al. 2017, Eq. 26), and is almost unchanged from Eq. (4) in the regimes we consider, as can be seen in Fig. 2.

4. EFFECT OF FLYBY ON THE OUTER PLANET

The goal of this section is to estimate the percentage of close encounters that can drive the outer planet into the ZLK window—which we will refer to as “successful flybys”. Recall that in our scenario the outer planet serves as a perturber that drives the inner planet into a high- e orbit. A successful flyby should raise significantly both the octupole parameter ε_{oct} (or eccentricity) and the inclination of the outer planet (Fig. 1). In the following, we will show that this is roughly equivalent to raising the inclination i_p to at least 48° .

The impact of a flyby on the outer planet depends on the dimensionless distance at closest approach $\tilde{q} \equiv q/a_p$, where q is the flyby periastron. For large \tilde{q} , we can average over time the orbit of the planet and the trajectory of the passing star and analytically compute the final inclination i_p and eccentricity e_p of the orbit of the outer planet (Heggie & Rasio 1996; Rodet et al. 2019). These analytical expressions hold only for $q \gtrsim 3a_p$, and the maximum inclination increase is about 6° , not enough for the system to enter the ZLK extreme eccentricity excitation window (which requires at least a misalignment of 48°). The impact of a flyby with a smaller periastron is chaotic and can only be studied numerically. We thus conduct N-body simulations with the IAS15 integrator of the REBOUND package (Rein & Liu 2012; Rein & Spiegel 2015). In order to limit the number of parameters, the simulations include two equal-mass stars $M_1 = M_2$ and a test particle (representing planet m_p). The integration time is chosen so that the distance between M_1 and M_2 is equal to $100q$ at the beginning and end of the simulations, and the time-step is adaptive.

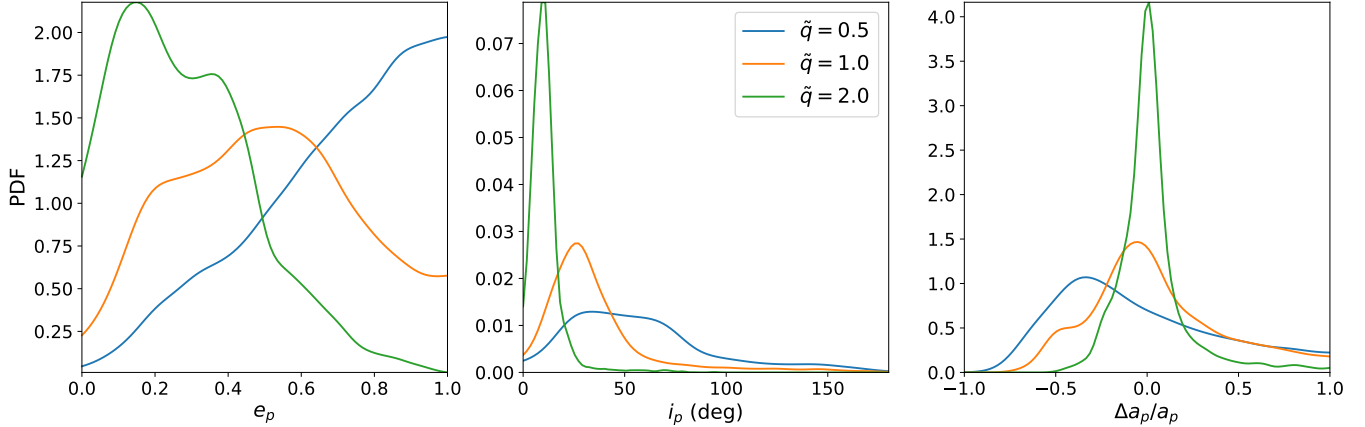


Figure 3. Probability distribution of the orbital elements (eccentricity, inclination and fraction change of semi-major axis) of the outer planet (m_p) after stellar flybys. Numerical results for three values of the pericenter distance q of the passing star are shown, with $\tilde{q} \equiv q/a_p = 0.5, 1$ and 2 . The planet is initially circular (and coplanar with the inner planet). Only the configurations where the planet remains bound are plotted here.

For star M_1 and M_2 approaching each other with relative velocity v_∞ (~ 1 km/s, typical of young clusters; see [Wright & Mamajek 2018](#)), the velocity at periastron q is given by

$$\begin{aligned} v_{\text{peri}}^2 &= v_\infty^2 + \frac{2GM_{\text{tot}}}{q} \\ &= v_\infty^2 + (10 \text{ km/s})^2 \left(\frac{50 \text{ au}}{q} \right) \left(\frac{M_{\text{tot}}}{2 M_\odot} \right), \end{aligned} \quad (10)$$

where $M_{\text{tot}} = M_1 + M_2$. For the regime we are considering, the gravitational focusing term dominates and v_∞ is negligible. This translates to a stellar eccentricity close to 1. In our simulations, we adopt $e = 1.1$ for all encounters. We have checked that the impacts of the flybys did not vary significantly with e as long as it remains close to 1.

In addition to the periastron distance q , a close encounter is specified by the inclination i between the flyby orbital plane and the initial orbital plane of the planet, and ω , the argument of periastron. Note that since the initial planetary orbit is circular, the outcome of an encounter does not depend on Ω , the longitude of node. Finally, the outcome of a flyby also depends on the phase of the planet λ_p at closest stellar approach.

In our simulations, we sample the periastron q over a uniform grid from $0.1a_p$ to $2a_p$, and choose

- ω with a flat prior between 0 and 2π ,
- i , with a $\sin(i)$ probability distribution, between 0 and π ,
- λ_p with a flat prior between 0 and 2π .

For each value of q , we sample $20 \times 20 \times 20$ angles (for ω , i , and λ_p) to determine the distributions of post-flyby

orbital parameters of the planet. Several examples of the post-encounter outcomes for three different \tilde{q} values are shown on Fig. 3. It is clear that flybys with $\tilde{q} = 2$ (and larger) produce a negligible number of systems with $i_p \gtrsim 40^\circ$. Thus, for our purpose, there is no need to consider encounters with $\tilde{q} > 2$.

Using results like Fig. 3, we can then compute, for each q , the percentage of systems that experience a successful flyby—i.e., the outer planet m_p remains bound and is in the eccentricity and inclination window (see Fig. 1) for inducing extreme eccentricity excitation of the inner planet (m_J) unaffected by the flyby. The resulting probability of successful flybys as a function of q is shown in Fig. 4 for $a_J/a_p = 0.1$ (the uncertainty in the probability due to the discrete sampling of the parameter space is of order 1%). In this case, $\varepsilon_{\text{oct}} > 0.05$ is equivalent to $e_p > 0.5$. Since a successful flyby would lead to the inner planet to migrate inward, we shall term this probability p_{mig} . We see from Fig. 4 that p_{mig} is approximately equal to the probability of producing high inclination: raising the inclination of the outer planet by 48° is the hardest constraint to get a successful flyby. This is in line with previous studies finding that the inclination is harder to raise than the eccentricity ([Li & Adams 2015](#); [Wang et al. 2020](#)). In fact, for the entire range of semi-major axis ratios that we study (Eq. 5), most of the cases with high inclinations have $\varepsilon_{\text{oct}} > 0.05$, so that the probability of a successful flyby is most constrained by the requirement of significant inclination excitation ($i_p \in [48^\circ, 132^\circ]$). Consequently, p_{mig} can be considered independent of a_J/a_p . Our result for $p_{\text{mig}}(\tilde{q})$ as depicted in Fig. 4 will enable us to derive the occurrence rate of

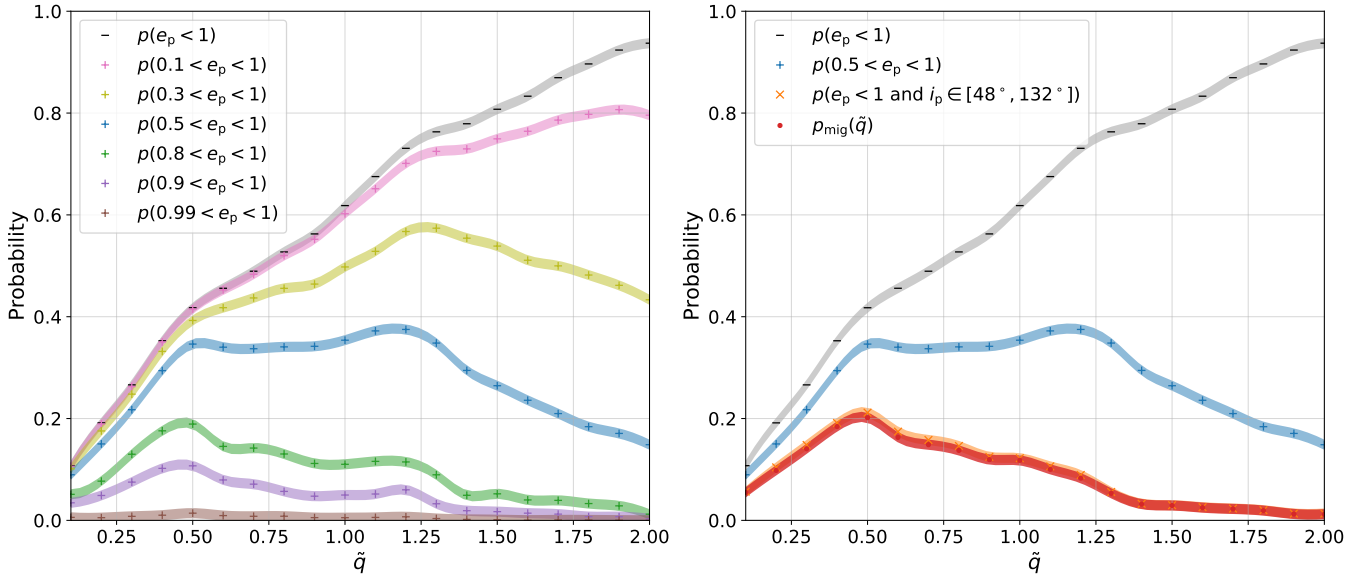


Figure 4. Various probabilities for the outer planet’s eccentricity e_p and inclination i_p to be in critical ranges after a stellar flyby, as functions of the dimensionless distance at the closest approach of the passing star, $\tilde{q} \equiv q/a_p$ (where a_p is the initial semi-major axis of the planet). The probabilities are computed numerically following the procedure described in Section 4. The red dots (right panel) show p_{mig} , which is the probability for the planet to be in the “extreme” ZLK window after a flyby, i.e. the outer planet reaches a sufficiently large inclination and eccentricity to drive the inner planet into high-e migration. This extreme ZLK window is approximately equivalent to $i_p \in [48^\circ, 132^\circ]$ and $\varepsilon_{\text{oct}} > 0.05$, the latter condition corresponds to $0.5 < e_p < 1$ for $a_J/a_p = 1/10$. Note that p_{mig} is almost equal to the probability that the outer planet reaches $i_p \in [48^\circ, 132^\circ]$ and remains bound ($e_p < 1$), indicating that the eccentricity condition is almost always met when the inclination condition is fulfilled.

successful flybys in Section 5, and to deduce the overall probability of forming HJs from close stellar encounters.

5. OCCURRENCE RATE

In this section, we estimate the occurrence rate of HJs that form in our flyby-induced high-e migration scenario (Section 2). This occurrence rate can be written as

$$\eta_{\text{HJ}} = t_{\text{cluster}} \eta_{\text{survival}} \int_{10 \text{ au}}^{300 \text{ au}} da_p \frac{d\eta_{\text{init}}}{da_p} \mathcal{R}_{\text{mig}}(a_p), \quad (11)$$

where $d\eta_{\text{init}}/da_p$ is the probability distribution function of the initial conditions (two planets, one giant planet around the snowline and one larger planet/perturber at a_p , with angular momentum ratio l less than 0.1), t_{cluster} is the lifetime of the birth cluster, η_{survival} is the probability for the giant planet to survive tidal disruption during high-e migration and \mathcal{R}_{mig} is the rate of close encounters that result in high-e migration. The lower limit of the a_p integration ensures dynamical stability, while the upper limit is the consequence of Eq. (5).

Tidal disruption can limit the efficiency of HJ formation through high-e migration. Using population synthesis models and analytical calculations (e.g.; Petrovich 2015b; Anderson et al. 2016; Muñoz et al. 2016; Teysandier et al. 2019; Vick et al. 2019), it has been

estimated that most of the giant planets that reach e_{lim} will be destroyed by the tidal forces of their host star. However, there are important uncertainties regarding the fraction of surviving planets, depending on the properties of tidal dissipation. Vick et al. (2019) showed that strong dissipation, through a mechanism called *chaotic tides*, can sometimes save planets otherwise fated for tidal disruption by rapidly decreasing their eccentricities. They estimated that $\eta_{\text{survival}} \sim 20\%$ of migrating planets could survive as HJs.

Observations provide only limited information on $d\eta_{\text{init}}/da_p$. Radial velocity surveys suggest an occurrence rate for giant planets between 10 and 30%, with a maximum likelihood around 3 au (e.g., Fernandes et al. 2019). On the other hand, direct imaging surveys point towards an occurrence rate of wide planetary/brown dwarf companions (10-300 au) of around 5-10% (Nielsen et al. 2019; Vigan et al. 2020). The correlation between the occurrences of giant planets at a few au and companions at 10–300 au is not known. Thus,

$$\eta_{\text{init}} \equiv \int_{10 \text{ au}}^{300 \text{ au}} da_p \frac{d\eta_{\text{init}}}{da_p} \sim 0.5 - 10\%. \quad (12)$$

The dependency of $d\eta_{\text{init}}/da_p$ on the semi-major axis a_p is unconstrained.

From Section 4, we can derive the rate of successful flybys, which lead to suitable conditions for HJ formation. This is a function of the cluster stellar density distribution $dn_*(v_\infty)$, which is a function of the velocity distribution f of the stellar velocities v_∞ . We take f to be a Maxwell-Boltzmann distribution with dispersion σ_* :

$$dn_* = n_* f(v_\infty) dv_\infty \quad (13)$$

$$f(v_\infty) = \sqrt{\frac{1}{\pi}} \frac{v_\infty^2}{\sigma_*^3} \exp\left(-\frac{v_\infty^2}{2\sigma_*^2}\right). \quad (14)$$

The cluster density n_* can take a wide range of values, from 10^{-1} stars/pc³ in the nearby OB associations to 10^6 stars/pc³ in the center of globular clusters. Moreover, in an unbound stellar association, which corresponds to most stellar birth environments, the density decreases with time. As a rough estimate, we suppose that our cluster of interest maintains a 10^3 stars/pc³ density for the first $t_{\text{cluster}} \sim 20$ Myr of its life (Pfalzner 2013). We suppose that the flyby rate at later times is negligible due to the much smaller density. The velocity dispersion σ_* is better constrained thanks to observations in nearby associations and cluster (e.g. Wright & Mamajek 2018). We adopt $\sigma_* \approx 1$ km/s. The rate of successful flybys is then:

$$\mathcal{R}_{\text{mig}}(a_p) = \int_0^\infty dn_*(v_\infty) v_\infty \int_0^{+\infty} \pi db^2(q, v_\infty) p_{\text{mig}}(\tilde{q}), \quad (15)$$

where p_{mig} is depicted in Fig. 4. The impact parameter $b(q, v_\infty)$ associated with an hyperbolic trajectory of periastron q and velocity at infinity v_∞ is:

$$b^2 = q^2 \left(1 + \frac{2GM_{\text{tot}}}{qv_\infty^2}\right) \approx \frac{2GM_{\text{tot}}q}{v_\infty^2}. \quad (16)$$

Using the result shown in Fig. 4, we find

$$\mathcal{R}_{\text{mig}} = \mathcal{R}_{\text{close}} \int_0^{+\infty} d\tilde{q} p_{\text{mig}}(\tilde{q}) \approx 0.15 \mathcal{R}_{\text{close}} \quad (17)$$

where

$$\begin{aligned} \mathcal{R}_{\text{close}} &\equiv 2\pi a_p GM_{\text{tot}} n_* \int_0^\infty \frac{dv_\infty}{v_\infty} f(v_\infty) \\ &= \frac{2\sqrt{2}\pi a_p GM_{\text{tot}} n_*}{\sigma_*} \\ &\approx 20 \left(\frac{n_*}{10^3 \text{ pc}^{-3}}\right) \left(\frac{M_{\text{tot}}}{2 M_\odot}\right) \left(\frac{a_p}{50 \text{ au}}\right) \\ &\quad \times \left(\frac{\sigma_*}{1 \text{ km/s}}\right)^{-1} \text{ Gyr}^{-1} \end{aligned} \quad (18)$$

is the rate of close encounters with periastron below a_p .

Combining Eqs. (11), (12), (17), and (18), we have

$$\begin{aligned} \eta_{\text{HJ}} &\approx 0.1\% \left(\frac{M_{\text{tot}}}{2 M_\odot}\right) \left(\frac{\langle a_p \rangle}{50 \text{ au}}\right) \\ &\quad \times \left(\frac{\eta_{\text{init}}}{10\%}\right) \left(\frac{\mathcal{R}_{\text{mig}}/\mathcal{R}_{\text{close}}}{15\%}\right) \left(\frac{\eta_{\text{survival}}}{20\%}\right) \\ &\quad \times \left(\frac{n_*}{10^3 \text{ pc}^{-3}}\right) \left(\frac{t_{\text{cluster}}}{20 \text{ Myr}}\right) \left(\frac{\sigma_*}{1 \text{ km/s}}\right)^{-1} \end{aligned} \quad (19)$$

where

$$\langle a_p \rangle \equiv \frac{1}{\eta_{\text{init}}} \int_{10 \text{ au}}^{300 \text{ au}} da_p \frac{d\eta_{\text{init}}}{da_p} a_p. \quad (20)$$

Equation (19) gives an estimate for the occurrence rate of HJs produced in our scenario, and illustrates its dependence on various uncertain parameters. Major uncertainties include η_{init} , the occurrence rate of the initial two-planet systems, and the density and lifetime of the birth clusters, the latter two may vary by orders of magnitude.

The observed occurrence rate of HJs around solar-type stars is 0.5–1% (e.g. Dawson & Johnson 2018). With the adopted fiducial parameters in Eq. (19), this formation channel can account for 10–20% of the observed HJ population. But with more optimistic n_* and t_{cluster} values, our estimated η_{HJ} can be compatible with the observed value.

6. SUMMARY AND DISCUSSION

6.1. Summary

In this paper, we have studied a new scenario for the formation of hot Jupiters (HJs) following a close stellar encounter—we call it “flyby Induced High-e Migration”. This could account for the recently observed correlation between the occurrence of HJs and stellar overdensities (Winter et al. 2020). In this scenario, we suppose that stellar flybys could excite the eccentricity and inclination of an outer planet or brown dwarf (at $a_p \sim 10$ –300 au), which would trigger the high-e migration of an inner cold Jupiter (initially at a few au). High-e migration requires the outer planet to be in a suitable window of inclination and eccentricity to induce extreme von Zeipel-Lidov-Kozai (ZLK) oscillations of the inner planet (Section 3). We carry out simulations of the secular evolution of two-planet systems to determine the require “migration” window driven by the octupole ZLK effect, extending previous test-particle results. Through extensive N-body numerical experiments, we find that for a stellar flyby to have a significant impact on the two-planet system (more specifically, to produce sufficient inclination and eccentricity in the outer planet, and thereby to trigger high-e migration of the inner

planet), its closest approach should be comparable to the semi-major axis of the outer planet. We then estimate the rate of such “successful” encounters and the likelihood that they will lead to the formation of HJs, taking into account geometric and stellar density parameters, as well as tidal disruption of migrating giant planets and the probability to have a suitable planetary system in the first place. Equation (19) gives the resulting occurrence rate of HJs produced in this scenario and its dependence on various parameters. Although the estimated occurrence rate relies on a few poorly constrained parameters, our analysis suggests that this HJ formation channel requires the birth cluster to retain a high stellar density for more than 20 Myr in order to account for a significant fraction of the observed HJ population.

6.2. Main Uncertainties

No further analysis or numerical simulations can significantly refine our estimate [Eq. (19)] until a better understanding on the properties of the typical stellar birth cluster is obtained, in particular the stellar density n_* as a function of time.

Furthermore, the correlation between cold Jupiters and more distant planets or brown dwarfs is currently unknown. So the occurrence rate of the two-giant-planet initial systems is not constrained. Our knowledge should improve with the next generation of exoplanet imaging surveys.

6.3. Comparison with other high- e migration paths

In the following we consider several other possible mechanisms for HJ formation. All of these are less promising for explaining the correlation between HJs and stellar overdensities reported by Winter et al. (2020).

6.3.1. Planet-planet scattering

Planet-planet scattering is another possible path to create high-eccentricity orbits, which could then lead to high- e migration of giant planets. Wang et al. (2020) determined that it could account for a significant formation of hot Jupiters in their simulations involving stellar flybys. This mechanism does not require raising the inclination of the outer planet to enter the ZLK regime, but only exciting the eccentricity enough to prompt a close encounter. How high the eccentricity needs to be raised depends on the semi-major axis ratio a_J/a_p . For $a_J/a_p = 0.5$, the required eccentricity for close planet-planet encounter is about 0.5, and we found from our flyby simulations that the probability can be $\sim 40\%$ for $\tilde{q} \lesssim 2$ (see Fig. 4). For $a_J/a_p = 0.1$, the required eccentricity is 0.9, and our simulations suggest a much

smaller probability ($\lesssim 10\%$; see Fig. 4). Note that as a general rule, we found that a flyby more readily raises the eccentricity than the inclination of the planet.

However, the probability that planet-planet scattering leads to HJ formation is likely much smaller. The eccentricity of the inner planet must increase sufficiently to enter the effective range of tidal dissipation, while remaining bound to the system. The outcome of an encounter between the planets varies with the conditions of the encounter and with the semi-major axis, divided between ejection, planet-planet merger, collision with the star and survival as a hot Jupiter. This problem has recently been studied in Li et al. (2021) for initially quasi-circular orbits. In their simulations, the probability that a planet undergoes a close encounter with the host star and becomes a HJ is less than 1%. Although in our case one of the planets has a highly eccentric orbit, the order of magnitude is likely similar. Thus, following a stellar flyby, planet-planet scattering seems unlikely to be more common than ZLK excitation to trigger high- e migration.

6.3.2. Stellar companion

The probability for a solar-type star to have a stellar companion at separations 100-1000 au is close to 20% in the field (Raghavan et al. 2010). Assuming a flat eccentricity and an “isotropic” inclination distributions, a significant fraction of binary companions could induce ZLK migration of giant planets. This HJ formation channel has been well studied in the literature (see Petrovich 2015b; Anderson et al. 2016; Muñoz et al. 2016; Vick et al. 2019, and references therein). The predicted HJ occurrence rate is of order 0.1-0.2%, with one of the main uncertainties being tidal disruption of the migrating planet. This formation channel seems more efficient at forming HJs because of the higher occurrence rate of stellar companions at large separation and, most importantly, because it does not require a flyby.

However, this formation channel struggles to account for the observed correlation between HJs and stellar overdensities (Winter et al. 2020). While the dependence of the stellar multiplicity on the stellar density is not well constrained, several surveys in nearby clusters seems to indicate that overdensity actually decreases stellar multiplicity (King et al. 2012; Marks & Kroupa 2012).

6.3.3. Tides from the stellar cluster

Stellar clusters create a global gravitational potential, which can trigger eccentricity and inclination variations on wide companions (Hamilton & Rafikov 2019a,b). Similar to the ZLK mechanism, here the “perturber” is the global potential of the cluster. For a planetary

system located at a distance R_c from the center of the cluster, the eccentricity excitation timescale is of order

$$T \sim \frac{R_c^3}{GM_c} n_p \sim \frac{3n_p}{4\pi G \bar{\rho}_*} \\ \sim 1 \text{ Gyr} \left(\frac{10^3 M_\odot / \text{pc}^3}{\bar{\rho}_*} \right) \left(\frac{50 \text{ au}}{a_p} \right)^{\frac{3}{2}} \left(\frac{M_1}{1 M_\odot} \right)^{\frac{1}{2}} \quad (21)$$

where n_p , a_p are the (initial) mean-motion and semi-major axis of the planet, M_c is the enclosed cluster mass at R_c and $\bar{\rho}_*$ the mean density of the cluster. This timescale is much larger than the lifetime of the cluster. Moreover, at such a density, about 20 close flybys are

expected to occur within 1 Gyr (Eq. 18), and their influence will be dominant on the dynamics of the planet.

ACKNOWLEDGEMENTS

This work has been supported in part by the NSF grant AST-17152 and NASA grant 80NSSC19K0444. YS is supported by the NASA FINESST grant 19-ASTRO19-0041. We made use of the PYTHON libraries NUMPY (Harris et al. 2020), SCIPY (Virtanen et al. 2020), and PYQT-FIT, and the figures were made with MATPLOTLIB (Hunter 2007).

REFERENCES

- Anderson, K. R., Lai, D., & Storch, N. I. 2017, MNRAS, 467, 3066, doi: [10.1093/mnras/stx293](https://doi.org/10.1093/mnras/stx293)
- Anderson, K. R., Storch, N. I., & Lai, D. 2016, MNRAS, 456, 3671, doi: [10.1093/mnras/stv2906](https://doi.org/10.1093/mnras/stv2906)
- Beaugé, C., & Nesvorný, D. 2012, ApJ, 751, 119, doi: [10.1088/0004-637X/751/2/119](https://doi.org/10.1088/0004-637X/751/2/119)
- Cai, M. X., Kouwenhoven, M. B. N., Zwart, S. F. P., & Spurzem, R. 2017, MNRAS, doi: [10.1093/mnras/stx1464](https://doi.org/10.1093/mnras/stx1464)
- Dawson, R. I., & Johnson, J. A. 2018, ARA&A, 56, 175, doi: [10.1146/annurev-astro-081817-051853](https://doi.org/10.1146/annurev-astro-081817-051853)
- Fabrycky, D., & Tremaine, S. 2007, ApJ, 669, 1298, doi: [10.1086/521702](https://doi.org/10.1086/521702)
- Fernandes, R. B., Mulders, G. D., Pascucci, I., Mordasini, C., & Emsenhuber, A. 2019, ApJ, 874, 81, doi: [10.3847/1538-4357/ab0300](https://doi.org/10.3847/1538-4357/ab0300)
- Gaia Collaboration, Brown, A. G. A., Vallenari, A., et al. 2018, A&A, 616, A1, doi: [10.1051/0004-6361/201833051](https://doi.org/10.1051/0004-6361/201833051)
- Hamilton, C., & Rafikov, R. R. 2019a, MNRAS, 488, 5489, doi: [10.1093/mnras/stz1730](https://doi.org/10.1093/mnras/stz1730)
- . 2019b, MNRAS, 488, 5512, doi: [10.1093/mnras/stz2026](https://doi.org/10.1093/mnras/stz2026)
- Harris, C. R., Millman, K. J., van der Walt, S. J., et al. 2020, Nature, 585, 357, doi: [10.1038/s41586-020-2649-2](https://doi.org/10.1038/s41586-020-2649-2)
- Heggie, D. C., & Rasio, F. A. 1996, MNRAS, 282, 1064, doi: [10.1093/mnras/282.3.1064](https://doi.org/10.1093/mnras/282.3.1064)
- Hunter, J. D. 2007, Comput Sci Eng, 9, 90, doi: [10.1109/MCSE.2007.55](https://doi.org/10.1109/MCSE.2007.55)
- King, R. R., Goodwin, S. P., Parker, R. J., & Patience, J. 2012, MNRAS, 427, 2636, doi: [10.1111/j.1365-2966.2012.22108.x](https://doi.org/10.1111/j.1365-2966.2012.22108.x)
- Kozai, Y. 1962, AJ, 67, 591, doi: [10.1086/108790](https://doi.org/10.1086/108790)
- Laughlin, G., & Adams, F. C. 1998, ApJL, 508, L171, doi: [10.1086/311736](https://doi.org/10.1086/311736)
- Li, D., Mustill, A. J., & Davies, M. B. 2020, MNRAS, 496, 1149, doi: [10.1093/mnras/staa1622](https://doi.org/10.1093/mnras/staa1622)
- Li, G., & Adams, F. C. 2015, MNRAS, 448, 344, doi: [10.1093/mnras/stv012](https://doi.org/10.1093/mnras/stv012)
- Li, J., Lai, D., Anderson, K. R., & Pu, B. 2021, MNRAS, 501, 1621, doi: [10.1093/mnras/staa3779](https://doi.org/10.1093/mnras/staa3779)
- Lidov, M. L. 1962, Planet. Space Sci., 9, 719
- Liu, B., Muñoz, D. J., & Lai, D. 2015, MNRAS, 447, 747, doi: [10.1093/mnras/stu2396](https://doi.org/10.1093/mnras/stu2396)
- Malmberg, D., Davies, M. B., & Heggie, D. C. 2011, MNRAS, 411, 859
- Marks, M., & Kroupa, P. 2012, A&A, 543, A8, doi: [10.1051/0004-6361/201118231](https://doi.org/10.1051/0004-6361/201118231)
- Muñoz, D. J., Lai, D., & Liu, B. 2016, MNRAS, 460, 1086, doi: [10.1093/mnras/stw983](https://doi.org/10.1093/mnras/stw983)
- Nagasawa, M., Ida, S., & Bessho, T. 2008, ApJ, 678, 498, doi: [10.1086/529369](https://doi.org/10.1086/529369)
- Naoz, S., Farr, W. M., & Rasio, F. A. 2012, ApJL, 754, L36, doi: [10.1088/2041-8205/754/2/L36](https://doi.org/10.1088/2041-8205/754/2/L36)
- Nielsen, E. L., De Rosa, R. J., Macintosh, B., et al. 2019, AJ, 158, 13, doi: [10.3847/1538-3881/ab16e9](https://doi.org/10.3847/1538-3881/ab16e9)
- Parker, R. J., & Quanz, S. P. 2012, MNRAS, 419, 2448, doi: [10.1111/j.1365-2966.2011.19911.x](https://doi.org/10.1111/j.1365-2966.2011.19911.x)
- Petrovich, C. 2015a, ApJ, 805, 75, doi: [10.1088/0004-637X/805/1/75](https://doi.org/10.1088/0004-637X/805/1/75)
- . 2015b, ApJ, 799, 27, doi: [10.1088/0004-637X/799/1/27](https://doi.org/10.1088/0004-637X/799/1/27)
- Pfalzner, S. 2013, A&A, 549, A82, doi: [10.1051/0004-6361/201218792](https://doi.org/10.1051/0004-6361/201218792)
- Raghavan, D., McAlister, H. A., Henry, T. J., et al. 2010, ApJS, 190, 1, doi: [10.1088/0067-0049/190/1/1](https://doi.org/10.1088/0067-0049/190/1/1)
- Rein, H., & Liu, S.-F. 2012, A&A, 537, A128, doi: [10.1051/0004-6361/201118085](https://doi.org/10.1051/0004-6361/201118085)
- Rein, H., & Spiegel, D. S. 2015, MNRAS, 446, 1424, doi: [10.1093/mnras/stu2164](https://doi.org/10.1093/mnras/stu2164)
- Rodet, L., Beust, H., Bonnefoy, M., et al. 2019, A&A, 631, A139, doi: [10.1051/0004-6361/201935728](https://doi.org/10.1051/0004-6361/201935728)

- Shara, M. M., Hurley, J. R., & Mardling, R. A. 2016, *ApJ*, 816, 59, doi: [10.3847/0004-637X/816/2/59](https://doi.org/10.3847/0004-637X/816/2/59)
- Teyssandier, J., Lai, D., & Vick, M. 2019, *MNRAS*, 486, 2265, doi: [10.1093/mnras/stz1011](https://doi.org/10.1093/mnras/stz1011)
- Vick, M., Lai, D., & Anderson, K. R. 2019, *MNRAS*, 484, 5645, doi: [10.1093/mnras/stz354](https://doi.org/10.1093/mnras/stz354)
- Vigan, A., Fontanive, C., Meyer, M., et al. 2020, arXiv e-prints, 2007, arXiv:2007.06573.
<http://adsabs.harvard.edu/abs/2020arXiv200706573V>
- Virtanen, P., Gommers, R., Oliphant, T. E., et al. 2020, *NatureMethods*, 17, 261, doi: [10.1038/s41592-019-0686-2](https://doi.org/10.1038/s41592-019-0686-2)
- von Zeipel, H. 1910, *Astronomische Nachrichten*, 183, 345, doi: [10.1002/asna.19091832202](https://doi.org/10.1002/asna.19091832202)
- Wang, Y.-H., Leigh, N. W. C., Perna, R., & Shara, M. M. 2020, *ApJ*, 905, 136, doi: [10.3847/1538-4357/abc619](https://doi.org/10.3847/1538-4357/abc619)
- Winter, A. J., Kruijssen, J. M. D., Longmore, S. N., & Chevance, M. 2020, *Nature*, 586, 528, doi: [10.1038/s41586-020-2800-0](https://doi.org/10.1038/s41586-020-2800-0)
- Wright, N. J., & Mamajek, E. E. 2018, *MNRAS*, 476, 381, doi: [10.1093/mnras/sty207](https://doi.org/10.1093/mnras/sty207)
- Wu, Y., & Lithwick, Y. 2011, *ApJ*, 735, 109, doi: [10.1088/0004-637X/735/2/109](https://doi.org/10.1088/0004-637X/735/2/109)
- Wu, Y., & Murray, N. 2003, *ApJ*, 589, 605, doi: [10.1086/374598](https://doi.org/10.1086/374598)